Tellus (1990), *42A*, 378–389

Can chaos and intransitivity lead to interannual variability?

By E. N. LORENZ, *Center for Meteorology and Physical Oceanography, Massachusetts Institute of Technology, Cambridge, MA 02139, USA*

(Manuscript received 8 November 1988; in final form 1 June 1989)

ABSTRACT

We suggest that the atmosphere–ocean–earth system is unlikely to be intransitive, i.e., to admit two or more possible climates, any one of which, once established, will persist forever. Our reasoning is that even if the system would be intransitive if the external heating could be held fixed, say as in summer, the new heating patterns that actually accompany the advance of the seasons will break up any established summer circulation, and an alternative circulation may develop during the following summer, particularly if chaos has prevailed during the intervening winter. We introduce a very-low-order geostrophic baroclinic "general circulation" model, which may be run with or without seasonal variations of heating. Under perpetual summer conditions the model is intransitive, admitting either weakly oscillating or strongly oscillating westerly flow, while under perpetual winter conditions it is chaotic. When seasonal variations of heating are introduced, weak oscillations prevail through some summers and strong oscillations prevail through others, thus lending support to our original suggestion. We develop some additional properties of the model as a dynamical system, and we speculate as to whether its behavior has a counterpart in the real world.

1. Introduction

The large-scale wind, temperature, and moisture patterns in the atmosphere, and the accompanying conditions in the underlying ocean and land surfaces, undergo variations on time scales ranging from days to aeons. The longer-period variations are frequently looked upon as changes in climate. As possible causes for these changes, climatologists have often invoked the presumed variations of certain external influences. By now there is considerable evidence that changing external conditions do play a significant role; this is particularly true of the earth's orbital parameters (cf. Imbrie, 1982). However, much of this evidence has only recently emerged, and the original reason for attributing internal changes to external changes must have been simply that external changes appeared capable of producing internal changes.

Recent numerical studies have uncovered a multitude of self-contained dynamical systems that undergo variations on a wide range of time scales, without the aid of any varying external influences. If apparent capability constitutes a rationale for pursuing a line of investigation, it behooves us to ask whether some climatic changes may be internally rather than externally produced, i.e., whether they are simply the natural internal oscillations that one would expect to find in something as intricate as the atmosphere–ocean–earth system. Of course the activity of this system requires external heating, ultimately derived from the sun, but this is not to say that *variations* in the system require *variations* in external heating. In this study we shall examine a mechanism that in theory can produce changes on time scales of years, with no variations in external conditions other than the normal seasonal cycle.

By a dynamical system, we sometimes mean any system whose exact present state completely determines its state at some time in the near future, according to a set of rules, whence, by extrapolation, in many instances at least, all future states are completely determined. Systems of this sort are most often defined by sets of differential or difference equations. Sometimes

we also include systems where the exact present state only approximately determines a near-future state; here there is no assurance that distant-future states will be even approximately determined. This extended definition admits many real physical systems, whose behavior commonly involves at least some randomness or uncertainty. Prominent among these systems is the atmosphere plus its immediate surroundings.

Dynamical-systems theory is principally concerned with infinite-term or very-long-term typical behavior. Often this is determined by the governing rules even when states at specific future times are not. For the atmosphere–ocean–earth system, which we may call the *climate system,* this behavior is synonymous with the climate.

Two properties that characterize some but not all dynamical systems are chaos and intransitivity. Neither property implies either the presence or the absence of the other. A chaotic system is one that exhibits sensitive dependence on initial conditions, i.e., where the approximate present state is insufficient to determine approximate states in the distant future, whether or not the exact present state determines the future. For such systems, any approximate repetition of previous behavior will be of temporary duration, and periodicity will not develop. Numerical values of any variable at equal widely spaced intervals, e.g., once-a-year observations of temperature at a particular weather station, will have the appearance of random numbers.

An intransitive system is one with a positive probability of acquiring any one of several sets of infinite-term properties. The particular set that becomes established will depend upon some initial state. In naturally occurring systems, where often no "initial" time is readily identifiable, it may effectively depend upon chance.

The climate system is unquestionably chaotic. It possesses obvious annual and diurnal periods, but, when these and their overtones and all other established or suspected periodic variations are subtracted out, a strong signal still remains. Further supporting evidence is the sensitive dependence on initial conditions exhibited by virtually all reasonably realistic atmospheric models. We do not know whether the system is intransitive, i.e., whether, if we could somehow stop the circulation and then let it resume, a different climate could develop. Some highly simplified atmospheric models are demonstrably intransitive (e.g., Budyko, 1969; Sellers, 1969), but the larger and more realistic models are not obviously so.

Some time ago, we proposed that the climate system was probably not intransitive (Lorenz, 1975). Our reasoning was as follows. Suppose that the system would be intransitive, with two possible climates, if the march of the seasons could be halted, say at northern-hemisphere summer. Suppose that in reality the system, with its seasons, develops a circulation compatible with one of these climates during a particular summer. This circulation will not persist, since the coming winter with its totally different solar-heating pattern will break it up. If the winter behavior is chaotic, the state at the onset of the next summer will effectively be selected at random, and the circulation that then develops may well be compatible with the alternative climate. The seasonal variations of solar heating will then have facilitated transitions from one climate to the other, i.e., they will have rendered the system transitive. What we will observe instead of intransitivity will be pronounced interannual variability.

The purpose of this paper is to demonstrate the reasonableness of this proposition in the context of a very simple model. We shall choose a model where the external thermal forcing varies with an annual period, and where chaos would prevail if the forcing were fixed at its winter intenity, while intransitivity would arise if it were fixed at its summer intensity. Verification of the hypothesis for the model will not, of course, tell us that a similar process takes place in the real climate system, but it will imply that any attempt to demonstrate that the real system is intransitive must not disregard the seasonal cycle.

2. The model

A model that we recently introduced as perhaps the simplest possible "general circulation" model (Lorenz, 1984; we shall refer to this paper as L84) will serve our present needs. The model equations are

$$dX/dt = -Y^2 - Z^2 - aX + aF, \tag{1}$$

$$dY/dt = XY - bXZ - Y + G, \tag{2}$$

$$dZ/dt = bXY + XZ - Z. \tag{3}$$

The variable X represents the strength of a large-scale westerly-wind current, and also the geostrophically equivalent large-scale poleward temperature gradient, while Y and Z are the strengths of the cosine and sine phases of a chain of superposed waves.

The quadratic terms containing the factor b represent the translation of the waves by the westerly current, while the remaining quadratic terms represent a continual transfer of energy, except when X become negative, from the westerly flow to the waves, which are assumed to tilt westward with height. The linear terms represent thermal and mechanical damping, and the constant terms represent thermal forcing. The equations were constructed in a somewhat *ad hoc* manner, but we noted in L84 that they could have been derived by extreme truncation of a geostrophic baroclinic model in spectral form.

We assume that $a < 1$ and $b > 1$. Two additional coefficients that ordinarily would have appeared have been reduced to unity by scaling t, X, Y, and Z. With this scaling a reasonable time unit is 5 days.

Since we found in L84 that eqs. (1)–(3) possess some chaotic solutions, we may suspect that only special solutions can be found by other than numerical means. For our present numerical integrations, we have used a fourth-order Taylor-series scheme, with a time increment Δt of 0.025 units or 3 h. With our chosen values of the coefficients we have encountered no oscillations with periods of less than 7 days, suggesting that our chosen Δt is sufficiently small.

As is customary in working with dynamical systems, we shall treat (X, Y, Z) as coordinates in a three-dimensional "phase space." A state of the system, defined by the values of X, Y, and Z, then becomes a point in the space, while a time-dependent solution becomes a trajectory or orbit. A point that is approached arbitrarily closely arbitrarily often by an orbit as $t \to \infty$ is an attracting point for that orbit. If a point is an attracting point for each of a set of orbits that together fill a finite volume, it is a point of an attractor.

From eqs. (1)–(3) we find that

$$d(X^2 + Y^2 + Z^2)/dt = -[a(2X - F)^2 + (2Y - G)^2 + (2Z)^2 - (aF^2 + G^2)]/2. \tag{4}$$

The right side of (4) vanishes on an ellipsoid E and is negative outside E. It follows that if S is any sphere centered at $(0, 0, 0)$ and completely enclosing E, all orbits passing through points outside S will ultimately penetrate S and then remain inside. Thus, as in many simple atmospheric models, the attractors, if they exist, are enclosed by an identifiable closed surface.

From (1)–(3), we also find that if V is the volume of an infinitesimal region,

$$dV/dt = V \operatorname{div}(dX/dt, dY/dt, dZ/dt) = -V(a + 2 - 2X). \tag{5}$$

The right side is negative only when $X < 1 + \frac{1}{2}a$. Thus, in contrast to many fully dissipative atmospheric models, where dV/dt is always negative, there is no assurance that small volumes will shrink to zero, and, in particular, that attractors will have zero volume. Likewise, there is no assurance that, if the direction of time is reversed, a small volume will expand toward infinity.

3. The model without seasons

Prior to examining solutions of eqs. (1)–(3) where F or G varies with an annual period, we shall consider solutions where F and G are constants; these are intended to model "perpetual winter" or "perpetual summer" conditions. We shall set $a = \frac{1}{4}$ and $b = 4$. In L84, with $F = 8$ and $G = 1$, we encountered chaos but found no evidence of intransitivity. We shall see that if instead $F = 6$ and $G = 1$, the system is intransitive but not chaotic.

Presumably F, representing the cross-latitude external-heating contrast, is greater in winter than in summer. We therefore identify $F = 8$ with a winter condition, and $F = 6$ with a summer condition. We could argue that G, which can logically represent the heating contrast between oceans and continents, should change sign from winter to summer, but we shall be content to vary F only.

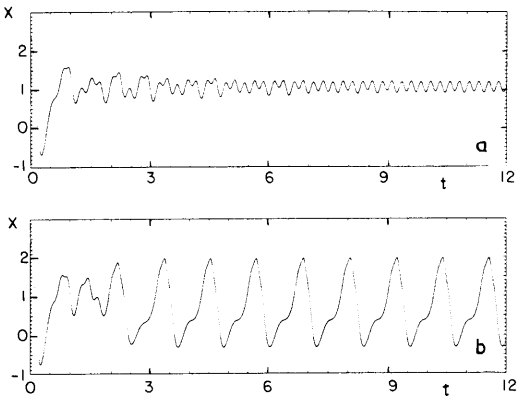

Fig. 1. (a) The variations of X (dimensionless) with t (months) in a numerical solution of eqs. (1)–(3), with $a = 0.25$, $b = 4.0$, $F = 6.0$, and $G = 1.0$ (summer conditions). The initial state is (2.4, 1.0, 0). (b) The same as Fig. 1a, except that the initial state is (2.5, 1.0, 0).

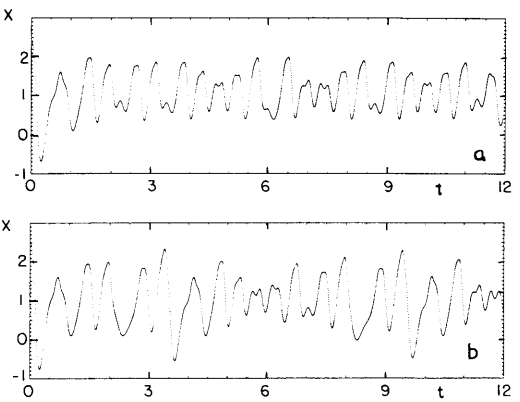

Fig. 2. (a) The same as Fig. 1a, except that $F = 8.0$ (winter conditions). (b) The same as Fig. 2a, except that the initial state is (2.5, 1.0, 0), as in Fig. 1b.

Fig. 1 shows the variations of X in two numerical solutions of (1)–(3) with $F = 6$, originating from the nearby points (2.4, 1.0, 0) and (2.5, 1.0, 0), and each extending for one year. During the first month, the two solutions look about alike, and each solution settles down after a few months of somewhat erratic behavior to periodic oscillations, but in the former case the oscillations have a much smaller amplitude and a much shorter period than in the latter. Extension of the solutions indicates that each type of oscillation, once established, is stable, and persists forever, so that the system is intransitive, while computations with other initial states reveal no further types of long-term behavior. We shall refer to the two types of activity as weak periodic oscillations and strong periodic oscillations.

Fig. 2 shows two solutions originating from the same states as in Fig. 1, but with $F = 8$. By two months the solutions have diverged, and they subsequently appear to vary chaotically. Extension of the solutions reveals no obvious differences in their long-term typical behavior, so that the system is presumably transitive as well as chaotic.

Since both periodic solutions with $F = 6$ are stable, the two attractors, which we shall call the weak attractor and the strong attractor, are simply the closed loops that a point traverses during a single period. The "weakness" of the weak attractor is not confined to the variations of X; nearby points are attracted to it relatively slowly. In Fig. 3, Y is plotted against $X + cZ$, with $c = -0.14$, for the two loops; this yields oblique projections on the X–Y-plane, like shadows on level ground when the sun is not directly overhead. We show each loop as a double curve, with the distance between the curves increasing linearly with Z, and thus indicating proximity to an observer above the X–Y-plane (if the Z-axis points upward).

The weak attractor appears as a simple quasi-ellipse, but in the more complicated strong attractor Y undergoes four oscillations between maxima and minima while X is undergoing one. We have avoided the more natural orthogonal projection ($c = 0$) because the weak attractor lies almost in a vertical plane, and would show up as a line segment instead of an ellipse.

The large dots mark the points where $Z = 0$, i.e., the intersections with the X–Y-plane. According to eq. (3), points move upward through the plane in the first and third quadrants and downward in the second and fourth. We note, perhaps surprisingly, that the two loops are linked together.

When $F = 8$, a projection of the attractor on the X–Y-plane would completely fill a region, and we show in Fig. 4 only the intersection of the attractor with the plane; this is to be compared with the ten dots in Fig. 3. The Cantor-set structure typical of "strange attractors" is apparent.

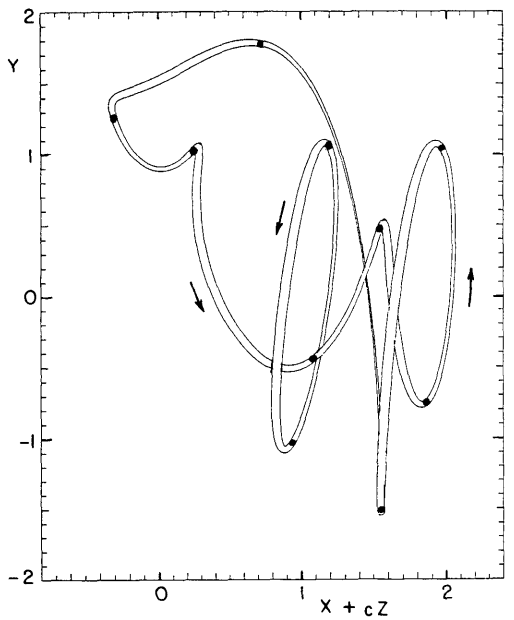

Fig. 3. Oblique projections of the two attractors (closed loops) of eqs. (1)–(3) on the plane $Z = 0$ for $a = 0.25$, $b = 4.0$, $F = 6.0$, and $G = 1.0$ (summer conditions), obtained by plotting Y against $X + cZ$, with $c = -0.14$. Each curve is represented by a pair of curves, with the distance between the curves of a pair proportional to $Z + 2.0$, and the true projection lying midway between the curves shown. Where two pairs of curves intersect, the pair with the lower value of Z has been broken. The large dots show the *intersections* of the attractors with the plane $Z = 0$. The arrows indicate the direction of flow along the loops.

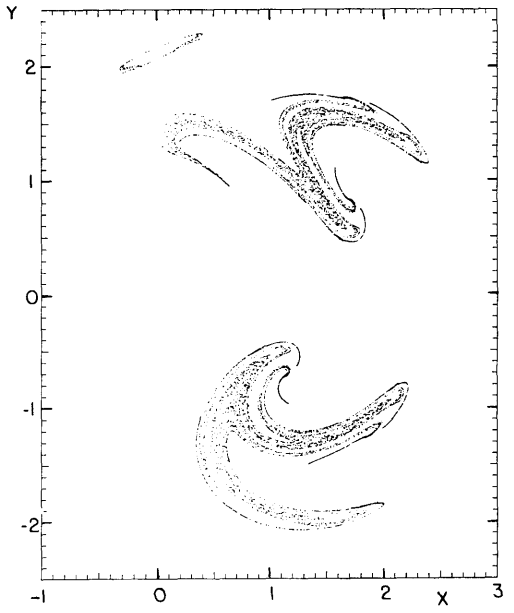

Fig. 4. The intersection of the attractor of eqs. (1)–(3) with the plane $Z = 0$, for $a = 0.25$, $b = 4.0$, $F = 8.0$, and $G = 1.0$ (winter conditions), as represented by 20,000 successive intersections of a single orbit.

Since the attractors of Fig. 3 must have separate basins of attraction, there must be a basin boundary or separatrix. By choosing initial states sufficiently close to the boundary, we could have postponed indefinitely the onset of periodic oscillations, thus producing an appearance of chaos. Likewise, the attractor of Fig. 4 contains within it a multitude of unstable periodic orbits, and, by choosing initial states sufficiently close to these, we could have postponed indefinitely the onset of irregular behavior, thus producing an appearance of periodicity and even intransitivity. The important point is that most choices of initial states in the regions covered by Figs. 3 and 4 will produce variations like those shown in Figs. 1 and 2.

In our main experiment, to be described in the following section, we shall allow F to vary sinusoidally, with a one-year period, between a minimum below 6.0 and a maximum above 8.0. If the types of behavior illustrated in Figs. 1 and 2 are to have any relevance to the experiment, each type should be representative of a considerable range of values of F, rather than ceasing as soon as F changes slightly from 6.0 or 8.0.

We are not particularly concerned with any alternative type of behavior that occurs only within a narrow range of F, since, in the main experiment, such behavior will probably not have time to become established before F moves out of the range. We are definitely interested in the moderately weak periodic behavior that replaces the truly weak oscillations after the latter undergo a period-doubling bifurcation at $F = 6.1$. Fig. 5, which is like Figs. 1 and 2 except that $F = 6.9$, illustrates the behavior. The upper curve again starts at (2.4, 1.0, 0), and the periodicity is fairly well established after one year. The lower curve starts at a point very close to the now unstable weakly oscillating solution, and, after two months, we see the even-numbered minima becoming successively weaker while the odd numbered minima become successively stronger,

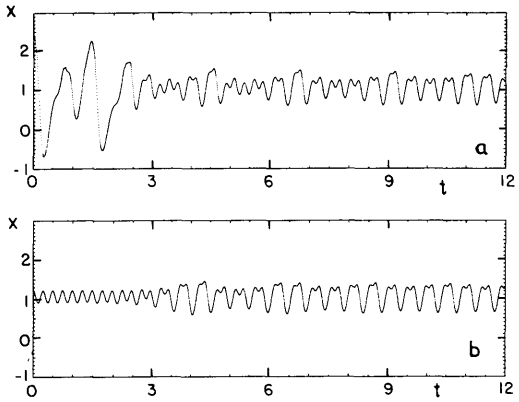

Fig. 5. (a) The same as Fig. 1a, except that $F = 6.9$. (b) The same as Fig. 5a, except that the initial state is (1.216, 1.147, 0), a point close to the unstable weakly oscillating periodic solution.

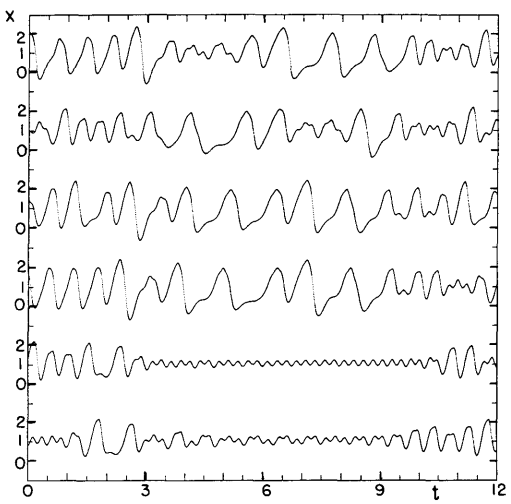

Fig. 6. The variations of X (dimensionless) with t (months) in a 6-year numerical solution of eqs. (1)–(3), with $A = 0.25$, $b = 4.0$, $F = 7.0 + 2.0\cos(2\pi t/\tau)$, and $G = 1.0$, where $\tau = 12$ months. Each row begins on 1 January, and, except for the first, each row is a continuation of the previous one.

until the dominant period is 15 days instead of 7.5.

If we regard the new type of behavior as a form of weak oscillation, we find that the intransitive periodic behavior occurring when $F = 6.0$ also occurs nearly everywhere between 5.2 and 6.9, while the transitive chaotic behavior found at 8.0 occupies the interval from 7.9 to 8.8. Below 5.2, and between 6.9 and 7.6, transitivity prevails, with only weak periodic fluctuations, while between 7.6 and 7.9 intransitivity reappears, with weak periodic or strong chaotic variations. A new type of strong periodic oscillation appears above 8.8. We should carefully note that these findings apply to the long-term behavior corresponding to *fixed* values of F.

In view of these findings, the most logical guess seems to be that the main experiment will exhibit chaos during the winters and some sort of periodicity during the summers. On the other hand, perhaps none of the types of behavior pictured in Figs. 1, 2, and 5 can become established before F changes signficantly. As with many nonlinear systems, there does not appear to be a simple line of reasoning that will decide between these alternatives, and, to determine what will happen, we must turn to the experiment itself.

4. The main experiment

As already noted, in our main experiment we shall let F vary sinusoidally while holding G fixed. For extreme values of F we choose 5.0 and 9.0, while $G = 1.0$. Under the assumption that the principal heating of the atmosphere comes from the underlying ocean and land rather than directly from the sun, while extreme conditions in the ocean and land lag behind the solstices, we could have let F assume its extreme values several weeks after the solstices, but for simplicity we shall let them occur at the beginning of January and July.

Fig. 6 shows the variations of X during 6 consecutive calendar years. Each winter except the sixth one begins with strong irregular fluctuations. During the first four summers the oscillations remain strong, although they become less rapid than in winter, but in the last two years weak fluctuations set in during the spring and persist into October. We shall refer to the two types of summer as active and inactive summers.

The occurrence of the 2 inactive summers could conceivably be a transient phenomenon, appearing before the system settles down to a regime where all summers are active, or perhaps even where all are inactive. To check on this possibility we have extended the solution to 100 years. A single quantity that readily distinguishes

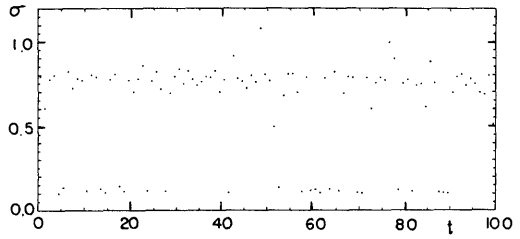

Fig. 7. The variations of σ (dimensionless) with t (years) in a 100-year numerical solution of eqs. (1)–(3), for the conditions of Fig. 6, where σ is the standard deviation of X within the period July through September.

the active from the inactive summers is the standard deviation σ of X within the 3-month period July through September. In Fig. 7 we show the 100 values of σ. Almost invariably $\sigma < 0.2$ or $\sigma > 0.5$; the distribution is clearly bimodal. Evidently active summers are far more frequent than inactive ones, and in one instance there are about 13 active summers in a row. A similar occurrence in the real world might easily, by the time the thirteenth active summer arrives, be interpreted as a climatic change.

Although we are dealing only with a model, we can consider it more likely that the qualitative results have some meaning if they continue to prevail for somewhat different values of the parameters. Accordingly, we have performed a number of 100-year runs, in each case after changing the mean value F_0 of F, the total range F' of F, or the fixed value of G.

We have started each run from the initial point (2.0, 1.0, 0), and have defined an inactive summer as one where $\sigma < 0.3$. With F' and G still equal to 4.0 and 1.0, and with F_0 equal to 8.0, 7.0, and 6.0, the number of inactive summers was respectively 10, 24, and 24. With $F_0 = 7.0$ and $G = 1.0$, while $F' = 5.0$, 4.0, 3.0, and 2.0, there were respectively 14, 24, 19, and 54 inactive summers. With $F_0 = 7.0$ and $F' = 4.0$, while $G = 1.0$, 0.9, 0.8, and 0.7, there were 24, 27, 62, and 93 inactive summers.

Any preference for active over inactive summers is therefore decidedly parameter-dependent. However, as to whether, in the context of a model, chaos and intransitivity can produce interannual variability, the answer is conclusively yes.

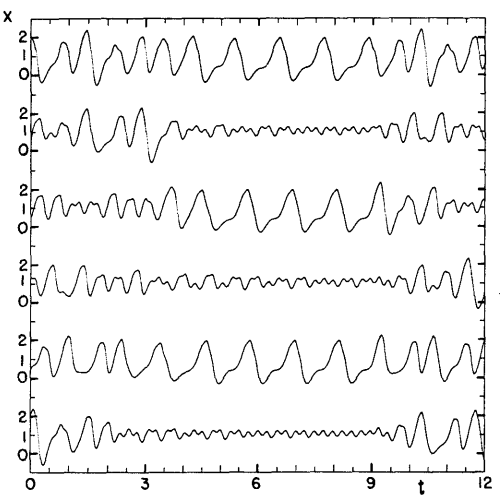

Fig. 8. The same as Fig. 6, except that $F = 8.0$ from October through March and $F = 6.0$ from April through September.

5. The modified experiment

Although the occurrence of both active and inactive summers in the main experiment may not surprise us, there was nevertheless no assurance, prior to the performance of the experiment, that both types would indeed be found. By making certain changes in the conditions of the experiment, without altering the spirit of the experiment, we can obtain rather similar results that, with the aid of a few reasonable assumptions, could have been anticipated. Instead of letting F vary sinusoidally, we shall simply hold F fixed at 8.0 from October through March, and at 6.0 from April through September.

Fig. 8 is the counterpart of Fig. 6 for the new experiment. Again the winters are chaotic, and both active and inactive summers occur. The most notable new feature is the uniformity of the variations during the latter parts of the active summers; they are all virtually identical to the strong periodic oscillations appearing in Fig. 1b. The important feature distinguishing one active summer from another is the phase of the oscillation.

Fig. 9 is the counterpart of Fig. 7. Again both types of summer continue to occur, with active summers predominating. The principal difference is the relative lack of variability of σ among the active summers.

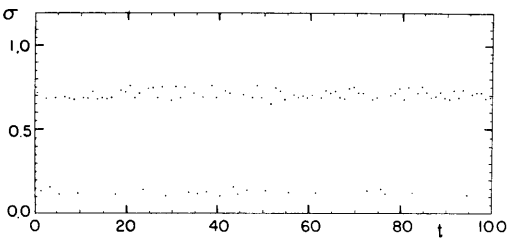

Fig. 9. The same as Fig. 7, except that F varies as in Fig. 8.

To account for our results, albeit in a non-rigorous manner, we assume first that by the end of any 6-month winter period, the state will have virtually reached the winter attractor. Any slight uncertainty as to the particular point on the attractor will result in an uncertainty in the phase of any periodic oscillations that develop during the following summer, so that the summer will end with comparable uncertainty, which will then amplify greatly during the ensuing chaotic winter. Hence the state at the end of the following winter will be virtually chosen at random from the winter attractor. The probability of a subsequent inactive summer should therefore approximately equal the probability that a randomly chosen point on the winter attractor lies in the basin of attraction of the weak summer attractor.

Since the loops that form the two summer attractors are linked together (see Fig. 3), we can expect that their basins of attraction will be somehow intertwined. Fig. 10 is a rather low-resolution picture of the intersections of the two basins, which we may call the weak basin and the strong basin, with the X–Y-plane; the weak basin is shaded and the strong basin is unshaded. To obtain the figure we have used each point of a grid of 180 × 180 points as an initial state for an integration with $F = 6.0$, and have continued each integration until one attractor or the other is approached.

We find that the structures of the basins are indeed complicated; this situation is apparently not unusual (cf. McDonald et al., 1985). Although each basin must form a connected set in three dimensions, the intersection of the weak basin with the plane contains several disjoint pieces.

In Fig. 11, a grid of 200 × 160 points covers a smaller area than that in Fig. 10, so that the resolution is somewhat higher. It is apparent that each basin possesses some fairly extensive continuous regions with fairly smooth boundaries, but there are also three elongated quasi-horizontal areas where neither plotted nor unplotted points predominate. Here the boundary, if it is smooth at all, can only be smooth on a very fine scale.

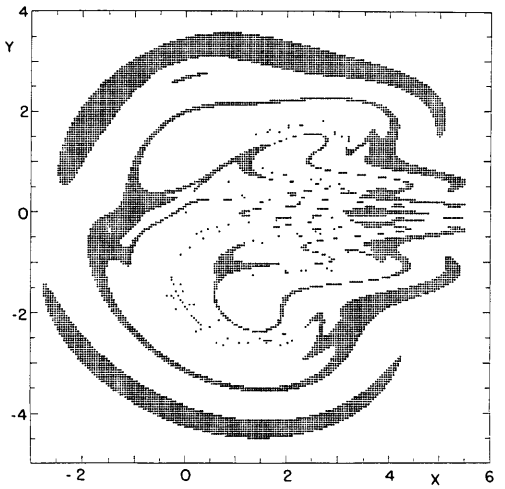

Fig. 10. The intersections of the basins of attractions of the two attractors of eqs. (1)–(3) with the plane $Z = 0$, for $a = 0.25$, $b = 4.0$, $F = 6.0$, and $G = 1.0$ (summer conditions), as resolved by points at intervals of 0.045 in the X- and Y-directions. The basin of the weak attractor is shaded and that of the strong attractor is unshaded.

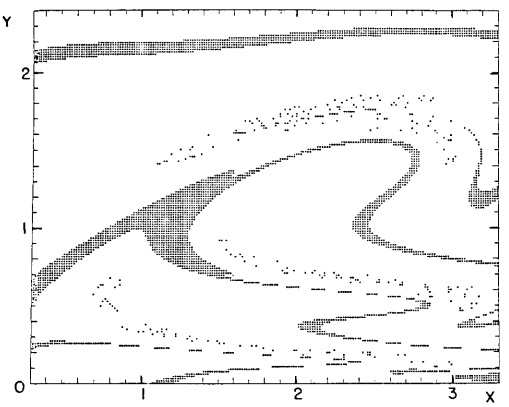

Fig. 11. An enlargement of a portion of Fig. 10, as resolved by points at intervals of 0.015 in the X- and Y-directions.

Comparing Fig. 4 with Fig. 10 or 11, we see that the intersection of the winter attractor with the X–Y-plane has points in common with the intersection of each summer basin with that plane. We would have obtained qualitatively similar results if instead of the X–Y-plane we had chosen other planes parallel to it; hence, in three dimensions, each summer basin contains a finite fraction of the points of the winter attractor. To estimate these fractions, we have performed a 5000-day integration with $F = 8.0$, starting at a point on the attractor, and have chosen the 1000 points occurring at 5-day intervals as initial states for integrations with $F = 6.0$, from which we have determined the basin in which each of the 1000 points lies. We find that 154 of them are in the basin of the weak attractor. For the ten separate sets of 100 consecutive points that make up the 1000-point set, the number of points in the weak basin ranges from 8 to 25.

Fig. 9, which exhibits 22 inactive summers, is consistent with this result. It would also appear that the 100 summers of Fig. 9 form an insufficient sample for a close estimate of the long-term probability of an inactive summer.

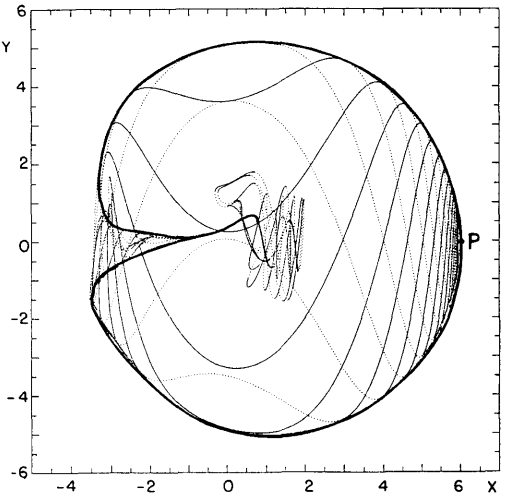

Fig. 12. Orthogonal projections of eight orbits emanating from P, the unstable fixed point (5.9933, −0.0083, 0.0399) of eqs. (1)–(3) on the plane $Z = 0$, for $a = 0.25$, $b = 4.0$, $F = 6.0$, and $G = 1.0$ (summer conditions). The orbits are shown as solid curves where $Z > 0$ and dotted curves where $Z < 0$. The separate orbits become indistinguishable near the strong attractor, which they approach. The heavy curve is an envelope of the projections.

6. The structures of the basins

In a model somewhat like the model of the modified experiment, but where the basins of the summer attractors are rather simple in structure, separated, perhaps, by an infinite plane or an ellipsoidal surface, it would be relatively easy for the winter attractor to lie entirely within one summer basin. In that case, the pronounced interannual variations would not develop. It is therefore of interest in the present case to look more closely at the structures of the basins, and the reasons why they are so complicated. In explaining the structures we shall have to invoke some dynamical-systems concepts that are not needed for an understanding of the previous sections.

Our first hint comes from Fig. 10, which suggests that the entire weak basin may lie no more than six units from the origin, so that all distant points will be attracted to the strong attractor. This proves to be the case. To demonstrate that this is so, we observe first that the system possesses a single fixed point P, where the right-hand sides of (1)–(3) vanish simultaneously, near $(F, 0, 0)$. This point possesses a one-dimensional stable manifold, consisting of two orbits converging upon P from opposite directions, and a two-dimensional unstable manifold U, made up of the orbits that emanate from P in all directions tangent to a particular plane. The manifold U lies inside the sphere S (see eq. (4)), and is shaped somewhat like the skin of an apple, but with the area farthest from the stem rounded off, and with the hole that contains the stem extending as a tube into the core, where it continues to meander. Fig. 12 is a special projection on the X–Y-plane. Eight orbits, emanating from P at 45-degree angles, are shown as thin solid curves where $Z > 0$ and dotted curves where $Z < 0$. Each orbit spirals outward from P, which is at the extreme right, and then spirals into the hole at the left. Using these orbits we have constructed the heavy curve, which passes through extreme values of Y, for given values of X, and also through extreme values of Y within the hole. The hole soon becomes very narrow, but maintains its existence as a hollow tube throughout its infinite length.

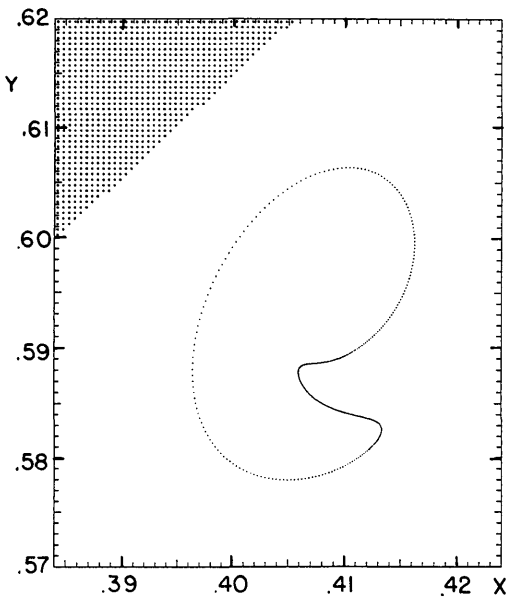

Fig. 13. The intersection of the unstable manifold of the fixed point of eqs. (1)–(3), with the plane $Z = 0$, for the conditions of Fig. 12, as resolved by the intersections of 400 orbits emanating from the fixed point (dotted closed curve), and portions of the intersections of the basins of attraction of the weak and strong attractors with the plane, as resolved by points at intervals of 0.0005 in the X- and Y-directions (shaded and unshaded areas).

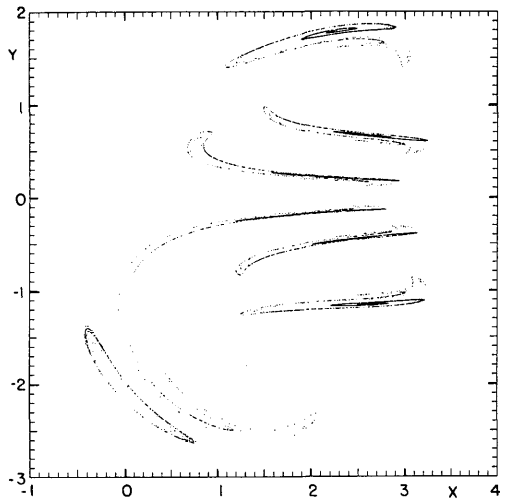

Fig. 14. The intersection of the repellor of eqs. (1)–(3) with the plane $Z = 0$, for the conditions of Fig. 10, as represented by 20,000 successive intersections of a single orbit running backward in time.

With the resolution of Fig. 12, the separate orbits that form the tube become indistinguishable as they reach positive values of X and subsequently approach the strong attractor. The distinctive shape of the attractor (compare Fig. 3) is easily discernible.

The significance of U is that since it is composed of orbits, no other orbit can cross it. Orbits coming from distant points therefore do not approach the general vicinity of their attractors from all directions, but must enter through the tube.

In Fig. 13, which shows a rather small region of the X–Y-plane, the shaded and unshaded areas, like those in Figs. 10 and 11, are intersections of the weak and strong basins with the region. The points that form the closed loop are the first intersections with the plane, within the tube, of 400 orbits emanating from P. It is apparent that although the tube passes rather close to the weak basin, it lies entirely in the strong basin, and so therefore do all orbits inside the tube. Orbits coming from distant points, other than a single orbit that stops at P, therefore all approach the strong attractor.

It follows that, if the direction of time is reversed, orbits in the weak basin cannot escape to infinity. What they do instead is to approach a reverse attractor, or "repellor." Fig. 14 shows the intersection of the repellor with the X–Y-plane, obtained in the same manner as Fig. 4, but with $\Delta t = -0.025$ and $F = 6.0$. Magnification, shown in Fig. 15, confirms the Cantor-set structure, whence the system with time reversed behaves chaotically.

As for orbits in the strong basin, some will escape to infinity if time is reversed, but some will not. The latter will approach a repellor, which proves to be the same as the repellor approached by orbits in the weak basin, shown in Figs. 14 and 15. Since orbits do not pass from one basin to the other, it follows that there are points of each basin arbitrarily close to each point of the repellor. The basin boundary therefore contains the repellor, in addition to the apparently smooth portions appearing in Figs. 10, 11, and 13. Thus, in the vicinity of the repellor, the two basins must be intricately intertwined.

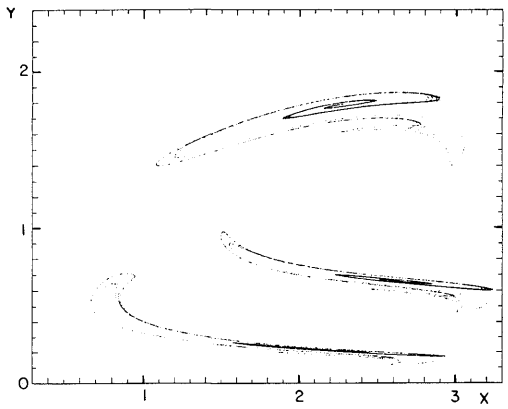

Fig. 15. An enlargement of a portion of Fig. 14, covering the same region as Fig. 11.

Comparison of Figs. 11 and 15, which cover the same area, shows that the elongated regions where neither basin appears to predominate coincide precisely with the strange repellor. The complicated structure of the basins is thus, in a certain sense, accounted for.

We complete our description of the two-way dynamical system by noting that the region at infinity is effectively a second repellor. Just as the boundary of the two basins of attraction contains the repellor, so the boundary of the two basins of repulsion, which consists of the manifold U and any points approached by orbits in U, contains the strong attractor.

7. Concluding remarks

We have constructed a simple atmospheric model that may be integrated numerically with or without seasonal variations of external thermal forcing. When the seasonal cycle is omitted, the system may be transitive or intransitive, and the behavior may be periodic or chaotic, depending upon the particular season that has been made permanent, but there is no sign of pronounced variations with periods of years or longer. When the seasonal cycle is included, strong interannual variations can occur, with irregular alternations between active summers, when the zonal westerly winds undergo strong oscillations, and inactive summers, when the oscillations are minor.

The mechanism that produces the year-to-year variations involves chaotic behavior during the colder months, which assures us that a virtually randomly chosen circulation pattern will be present when the warmer months begin. This allows one possible persistent circulation pattern to develop during one summer, while an alternative pattern may develop during another.

In view of the extreme crudeness of our model, it is reasonable to ask whether our results have anything to do with the real climate system. We believe that they may, although our reasoning is necessarily speculative.

First of all, we think that the real climate system would be chaotic if the external heating could be held fixed with its winter distribution (or that of any other season). We consider it far less likely that the system would be intransitive if the heating were fixed with its summer distribution (or that of any other season). However, we believe that it does not really matter whether there are two summer circulation patterns, each of which would persist forever if the heating could be held fixed, or whether there are simply two patterns that would be likely to persist for a few months. In either event, what would finally break up the summer circulation pattern would be the new heating distribution that would arrive with autumn. For that matter, it is immaterial whether the winter behavior is truly chaotic, or whether there is simply a tendency for irregular oscillations to prevail for a few months before periodic behavior sets in, as, for example, in the first few months in Fig. 5a. In either event a more or less randomly selected pattern will be present when summer begins.

Real atmospheric circulation anomalies often persist for many weeks, bringing heat waves or cold waves, or floods or droughts, to particular places. These places are different on different occasions. It seems likely that, in some cases, what is responsible for the eventual break-up of the anomaly is the march of the seasons, which brings new heating distributions with which the present circulation anomalies are incompatible. The seasonal variations of heating may therefore play a role that is quite distinct from their obvious role in producing different climatological normal conditions at different seasons.

Wholly aside from matters of climatological interest, we have found a rather striking

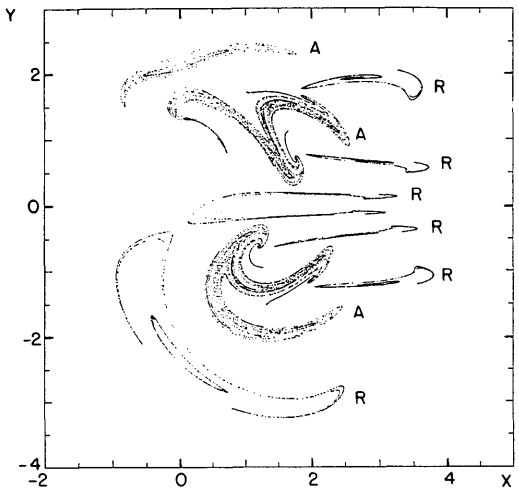

Fig. 16. The intersections of the attractor (pieces labeled A) and the repellor (pieces labeled R) of eqs. (1)–(3) with the plane $Z = 0$, for $a = 0.25$, $b = 4.0$, $F = 8.0$, and $G = 1.25$.

dynamical system that merits further study. It is semi-dissipative, i.e., infinitesimal volumes can either contract or expand, but in the long run they undergo net contraction, so that the attractors are sets of zero volume. Moreover, the system remains semi-dissipative when time is reversed; again there is net contraction, and the repellor is a set of zero volume.

We have subsequently found some values of the parameters for which both the attractor and the repellor are strange; we offer Fig. 16 as an example. We note that the attractor and the repellor carefully avoid one another. The generality of this observation merits considerable thought; according to Mestel (1987, private communication), it may depend upon the manner in which one chooses to define an attractor.

8. Acknowledgement

This work has been supported by the Climate Dynamics Program of the Atmospheric Sciences Section of the National Science Foundation, under Grant ATM-8515010.

REFERENCES

Budyko, M. I. 1969. The effect of solar radiation variations on the climate of the earth. *Tellus 21*, 611–619.

Imbrie, J. 1982. Astronomical theory of Pleistocene ice ages: a brief historical review. *Icarus 50*, 408–422.

Lorenz, E. N. 1975. Nondeterministic theories of climatic change. *Quaternary Research 6*, 495–506.

Lorenz, E. N., 1984. Irregularity: a fundamental property of the atmosphere. *Tellus 36A*, 98–110.

McDonald, S. W., Grebogi, C. Ott, E. and Yorke, J. A. 1985. Fractal basin boundaries. *Physica 17D*, 125–153.

Sellers, W. D. 1969. A global climate model based on the energy balance of the earth–atmosphere system. *J. Appl. Meteorol. 8*, 392–400.